Original Paper

Brain, Behavior and Evolution

Brain Behav Evol
DOI: 10.1159/000478738

Received: April 18, 2017
Returned for revision: June 3, 2017
Accepted after revision: June 15, 2017
Published online: September 5, 2017

Evidence for Concerted and Mosaic Brain Evolution in Dragon Lizards

Daniel Hoops[a] Marta Vidal-García[a] Jeremy F.P. Ullmann[b] Andrew L. Janke[b] Timothy Stait-Gardner[c] David A. Duchêne[d] William S. Price[c] Martin J. Whiting[e] J. Scott Keogh[a]

[a]Division of Ecology and Evolution, Research School of Biology, The Australian National University, Acton, ACT, [b]Centre for Advanced Imaging, The University of Queensland, Brisbane, QLD, [c]Nanoscale Organization and Dynamics Group, School of Science and Health, Western Sydney University, Penrith, NSW, [d]School of Life and Environmental Sciences, University of Sydney, and [e]Department of Biological Sciences, Discipline of Brain, Behaviour and Evolution, Macquarie University, Sydney, NSW, Australia

Keywords

Telencephalon · Diencephalon · Mesencephalon · Optic tectum · Tegmentum · Rhombencephalon · Cerebellum · Magnetic resonance imaging · Cognition · Reptile · Lizard · Concerted evolution · Mosaic evolution · Ecomorph

Abstract

The brain plays a critical role in a wide variety of functions including behaviour, perception, motor control, and homeostatic maintenance. Each function can undergo different selective pressures over the course of evolution, and as selection acts on the outputs of brain function, it necessarily alters the structure of the brain. Two models have been proposed to explain the evolutionary patterns observed in brain morphology. The concerted brain evolution model posits that the brain evolves as a single unit and the evolution of different brain regions are coordinated. The mosaic brain evolution model posits that brain regions evolve independently of each other. It is now understood that both models are responsible for driving changes in brain morphology; however, which factors favour concerted or mosaic brain evolution is unclear. Here, we examined the volumes of the 6 major neural subdivisions across 14 species of the agamid lizard genus *Ctenophorus* (dragons). These species have diverged multiple times in behaviour, ecology, and body morphology, affording a unique opportunity to test neuroevolutionary models across species. We assigned each species to an ecomorph based on habitat use and refuge type, then used MRI to measure total and regional brain volume. We found evidence for both mosaic and concerted brain evolution in dragons: concerted brain evolution with respect to body size, and mosaic brain evolution with respect to ecomorph. Specifically, all brain subdivisions increase in volume relative to body size, yet the tectum and rhombencephalon also show opposite patterns of evolution with respect to ecomorph. Therefore, we find that both models of evolution are occurring simultaneously in the same structures in dragons, but are only detectable when examining particular drivers of selection. We show that the answer to the question of whether concerted or mosaic brain evolution is detected in a system can depend more on the type of selection measured than on the clade of animals studied.

KARGER

E-Mail karger@karger.com
www.karger.com/bbe

Daniel Hoops
Department of Psychiatry and Douglas Hospital Research Centre
McGill University, 6875 Blvd LaSalle
Montreal, QC, H4H 1R3 (Canada)
E-Mail daniel.hoops@mail.mcgill.ca

Introduction

A relatively large and complex brain is one of the major characteristics of vertebrate animals, and this characteristic is linked to the diverse sensory, behavioural, social, and cognitive functions vertebrates display [Butler and Hodos, 2005]. Brains perform so many functions because they comprise many functionally distinct but interconnected structures that execute a wide array of disparate tasks [Kandel, 2013]. It may be that evolution does not select upon the brain as a whole, but rather that each functionally distinct structure is under different selective pressures with the result that different brain structures evolve independently. This is the mosaic brain evolution hypothesis [Striedter, 2005]. Alternatively, because brain regions are physiologically and developmentally interconnected, they may not be free to evolve independently and, instead, evolve in coordination in response to a "net" selective pressure. This is the concerted brain evolution hypothesis [Striedter, 2005; Finlay et al., 2011].

How free are different brain regions to respond individually to specific selection pressures, and how constrained are they to evolve as a single unit? The answer may be influenced by phylogeny. In mammals, the volumes of the major brain subdivisions appear to be evolving primarily in concert [Finlay and Darlington, 1995; Whiting and Barton, 2003; Striedter, 2005] whereas in birds, the major brain subdivisions seem to be evolving as a mosaic [Boire and Baron, 1994; Iwaniuk et al., 2004]. However, all groups show evidence of both processes, since there is also evidence for mosaic brain evolution in mammals [Barton and Harvey, 2000; Brown, 2001; Dobson and Sherwood, 2011; Hager et al., 2012] and concerted brain evolution in birds [Charvet et al., 2011; Gutiérrez-Ibáñez et al., 2014]. This dichotomy also exists between the major clades of fishes, with cartilaginous fishes primarily showing a concerted pattern of brain evolution [Yopak et al., 2010] whereas bony fishes seem to primarily exhibit a mosaic pattern [Kotrschal et al., 1998; Gonzalez-Voyer et al., 2009]. Though both evolutionary patterns occur together, it is generally thought that certain structures within the brain are driven by mosaic brain evolution, while others are driven by concerted evolution [Platel, 1976; Gutiérrez-Ibáñez et al., 2014]. A key question remains as to whether, and how, both patterns can interact to drive the evolution of a single brain structure.

The most closely related species-rich vertebrate group to birds and mammals is the squamate reptiles (snakes and lizards), and this makes them an ideal group for examining conditions which might favour concerted or mosaic modes of brain evolution. However, brain evolution in reptiles is poorly understood relative to other vertebrate groups. To date, the only study to look at the scaling of the major neural subdivisions across squamates found qualitative evidence for both concerted and mosaic brain evolution, but did not perform formal analyses [Platel, 1976]. There is evidence for mosaic brain evolution in lizards at the level of individual brain nuclei [ten Donkelaar, 1988; Lanuza and Halpern, 1997; Northcutt, 2013; Hoops et al., 2016], but none of these studies has examined evolution at the level of the major brain subdivisions. The only 2 studies [Powell and Leal, 2012, 2014] to have quantitatively examined the evolution of the major brain subdivisions across multiple reptile species found concerted evolution with respect to body size but no other evidence of brain evolution.

Each of the species that comprise the Australian semiarid agamid genus *Ctenophorus* (referred to as "dragons" [Hamilton et al., 2015]) can be allocated to 1 of 3 ecological groups, referred to as "ecomorphs": species that shelter in burrows "burrowers," those that shelter in rock crevices "rock dwellers," and those that shelter in grass hummocks "sprinters" [Greer, 1989; Melville et al., 2001]. Each ecological group is associated with a characteristic morphology [Greer, 1989; Thompson and Withers, 2005b]. Burrowers have short, stout limbs for digging and short tails to make a quick retreat; rock dwellers have dorso-ventrally flattened bodies and heads to squeeze into tight spaces; and sprinters have long legs and tails that allow them to make quick dashes back to the nearest grass hummock [Greer, 1989; Thompson and Withers, 2005b].

Given that selection has acted on habitat preference and body morphology to drive phenotypes towards particular ecomorphs, we hypothesized that selection may also affect brain morphology. We tested this hypothesis in a phylogenetic framework by means of a thorough examination of *Ctenophorus* brain morphology. This was done using 14 species from the central netted dragon (*C. nuchalis*) sp. group, such that every major clade within this species group was sampled [Greer, 1989; Melville et al., 2001; Chen et al., 2012].

We tested for changes in the brain as a whole and as a set of distinct subdivisions. We examined whether mosaic evolution, concerted evolution, or a combination of the two best explains variation in *Ctenophorus* brains between species. Furthermore, we addressed whether we can differentiate brain evolution in response to 2 disparate selection pressures occurring simultaneously in the same brain structures.

Materials and Methods

Specimen Acquisition

We collected 287 lizards from 14 *Ctenophorus* sp. from the wild in Australia (electronic supplementary material ESM 1; see www.karger.com/doi/10.1159/000478738 for all online suppl. material). All lizards were then transported to the Australian National University in Canberra, ACT, Australia, where they were maintained in outdoor enclosures. They were provided ad libitum access to water, opportunistic access to food (wild insects), and this diet was supplemented twice weekly with domestic crickets. The University's Animal Experimental Ethics Committee approved all research (protocol No. A201149).

Measuring Body Morphology

For each lizard, we measured 11 body regions: snout-to-vent length (SVL), front 4th-toe length, front palm length, front forearm length, front upper arm length, interlimb length, hind 4th-toe length, hind palm length, hind forearm length, hind upper arm length, and tail length, to the nearest millimeter using a transparent ruler. The 4th toe was chosen because it is the longest, and has been used previously in morphological studies of *Ctenophorus* lizards [Thompson and Withers, 2005a, b, c]. We measured head length, head width, and hip height to the nearest 0.01 millimetre with digital calipers and weight to the nearest 0.01 gram with a digital scale. All measurements were taken by D.H. and from the animal's left side for consistency (ESM 1: species means).

Calculating Brain Volumes with Magnetic Resonance Imaging

Each lizard was euthanized and perfused as described in Hoops [2015]. Magnevist (gadopentate dimeglumine, Bayer) was added to the fixative perfusate and storage buffer at a concentration of 0.1%, to maximize image contrast in magnetic resonance imaging (MRI) [Ullmann et al., 2010]. We did not dissect out the olfactory bulbs. After dissection, brains were stored at 4°C in a solution of 0.1% Magnevist and 0.05% sodium azide in PBS until imaging.

Whole-brain images were acquired using a Bruker Avance 11.74-tesla wide-bore spectrometer (Ettlingen, Germany) with a micro (2.5) imaging probe capable of generating magnetic gradients of 1.50 T/m. Parameters used in the scans were optimized for grey-to-white matter contrast in the presence of Magnevist. We used a fast, 3-dimensional (3D) gradient echo (T2-weighted) sequence (FLASH): repetition time = 40 ms, echo time = 8 ms, field-of-view = 11 × 11 × 16 mm, and matrix size = 110 × 110 ×160, which produced an image with 100-μm^3 isotropic voxels.

A minimum deformation model was built for each species, using, on average, 20 individuals per species (range 17–29; ESM 1), including approximately equal numbers of males and females. Our sample sizes were not sufficient to produce separate models for each sex, and so sexual dimorphism is not covered in this study. Appropriate sample sizes were determined empirically during the model-generation process according to previously defined criteria [Ullmann et al., 2015]. To create the models, the images were first cropped, re-oriented to a standard rostro-caudal orientation, and then manually masked, such that consistent coverage of the brain structures and nerve endings was achieved. The masked areas were set to the background value such that they were not included in subsequent calculations. All images were then B_0 intensity inhomogeneity-corrected, using the N3 algorithm [Sled et al., 1998]. An image with a good signal-to-noise ratio and no obvious artefacts was then manually selected from each group and used as an initial model for that group after blurring. All images within the respective groups were then recursively matched to their own evolving model of average structure to create a minimum deformation average, with a resulting resolution of 40 μm. The details of the model creation process can be found in Janke and Ullmann [2015]. The fitting stages in this case started at a resolution of 1.28 mm and finished with a resolution of 80 μm. Analyses were conducted using the 3D volumetric measure of voxel (the equivalent of a 3D pixel) counts, which can posteriorly be converted to millilitres by multiplying by 6.4×10^{-5}.

To look for both concerted and mosaic evolution in the lizard brain, we examined the volumes of the whole brain and the 6 subdivisions. These subdivisions are: the 2 divisions of the prosencephalon, the telencephalon and diencephalon, the 2 divisions of the mesencephalon, the tectum and tegmentum, and the 2 divisions of the rhombencephalon, the cerebellum and the remaining rhombencephalon (the metencephalon and mylencephalon, which are not easily distinguished in reptiles). It is at this level that evidence for both mosaic and concerted brain evolution has been found in avian reptiles [Iwaniuk et al., 2004] and proposed in squamate reptiles [Platel, 1976].

In order to measure the volumes of the 6 subdivisions in each of the models in an automated fashion, we used model-based segmentation. First, a global model of the tawny dragon (*C. decresii*) brain was created, and the 6 subdivisions were traced [Janke, and Ullmann, 2015]. Tracing was achieved first by using the interpolation function of the program Amira (Fischer 3D), followed by manual correction of every slice in all 3 dimensions, resulting in one 3D label for each subdivision of the tawny dragon MRI model (this process is called manual segmentation). There is no neuroanatomical atlas available for an agamid brain, so we analysed numerous available atlases for the brains of other lizards in order to accurately delineate the 6 subdivisions [ten Donkelaar, 1998; Del Corral et al., 1990; Medina et al., 1992; Greenberg, 1982; Smeets et al., 1986; Northcutt, 1967; Ulinski and Peterson, 1981; Butler and Northcutt, 1973; Cruce, 1974; Cruce and Newman, 1981; Schwab, 1979; Wolters et al., 1985; Wolters et al., 1984; ten Donkelaar et al., 2012]. Briefly, the telencephalon-diencephalon boundary is marked by the preoptic area and the epithalamus, the diencephalon-mesencephalon boundary by the pretectal nuclei, and the mesencephalon-rhombencephalon boundary by the isthmus. The optic tectum and cerebellum are cohesive, well-defined structures (Fig. 1).

We then created a global model for each of the remaining 13 *Ctenophorus* sp. [Janke and Ullmann, 2015]. Each species model was nonlinearly aligned to the tawny dragon model, using the same fit parameters as used to build the models [Janke and Ullmann, 2015]. The manually traced 3D labels for the tawny dragon model were back-transformed to each of the other species models (this process is called automatic segmentation) [Collins et al., 1994]. Visual inspection during the creation and alignment of the model and label during the back-transformation processes ensured that there were no obvious computational errors or misalignments. We then counted the number of voxels in each of the back-transformed labels to determine the volume of each subdivision for each species.

Statistical Analyses

Phylogenetic information, including relationships among species and branch lengths, was taken from a published time-calibrat-

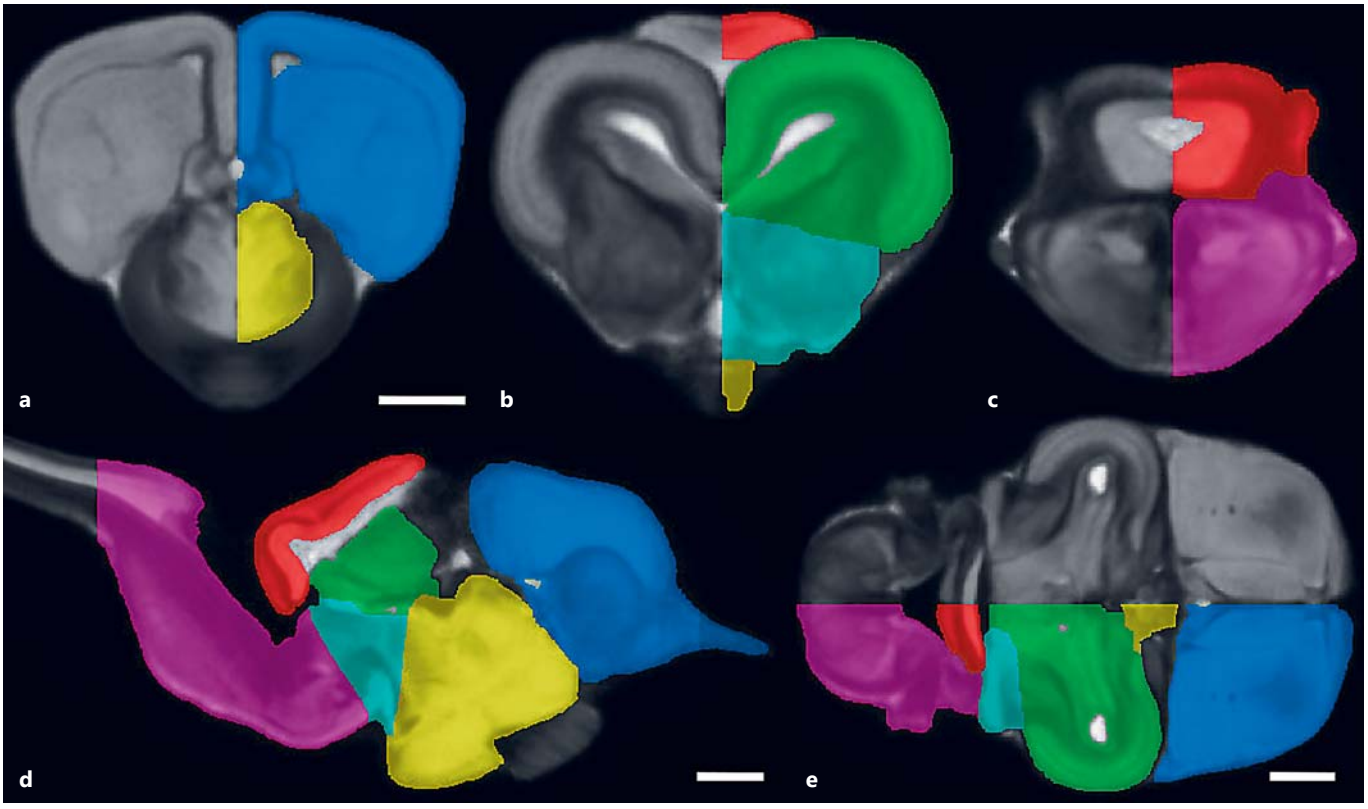

Fig. 1. The delineations of the 6 neural subdivisions superimposed on the MRI model of the tawny dragon (*Ctenophorus decresii*) brain. Anterior-posterior left-to-right coronal sections (**a–c**), a sagittal section (**d**), and a horizontal section (**e**) of the MRI atlas have been labelled with the 6 neural subdivisions. Blue, telencephalon; yellow, diencephalon; green, optic tectum; aqua, mesencephalon; red, cerebellum; purple, rhombencephalon. Scale bars, 1 mm.

ed molecular phylogenetic estimate [Chen et al., 2012]. We pruned this inferred phylogeny using the R [R Core Team, 2014] package *ape* [Paradis et al., 2004], in order to obtain a resulting tree with only the 14 *Ctenophorus* sp. used in this study.

Prior to conducting phylogenetic comparative analyses, for each subdivision, we compared the corrected Akaike information criterion (AIC) values according to Brownian motion, Ornstein-Uhlenbeck (OU), early-burst, kappa, and white noise (the absence of phylogenetic signal) models of brain evolution using the R packages *geiger* [Harmon et al., 2008] and *ouch* [Butler et al., 2004]. We considered the possibilities of brains evolving towards a single optima and 3 optimas (1/ecomorph) within the OU model (OU1 and OU3, respectively). The model of brain evolution that fit our data best, determined with AIC, was used as the model of brain evolution in subsequent phylogenetic comparative analyses. We also calculated rates of morphological evolution for all the brain variables and the external body measurements, in order to compare them using the R package *geomorph* [Adams and Otárola Castillo, 2013] and following the procedure of Denton and Adams [2015]. We used: (a) all brain and body variables, (b) overall brain size and SVL (a proxy for body size), and (c) size-corrected brain and body variables. All variables were normalized and centred prior to simulation, so that all means were equal to zero and all standard deviations were equal to one.

We then used phylogenetic linear models to determine whether the volume of each brain subdivision correlated with the brain volume across species. Previously, we [Hoops et al., 2016] (and others [Powell and Leal, 2012]) used standard major axis regressions for this type of analysis, but recent evidence suggests that linear models are the preferred statistical method [Kilmer and Rodríguez, 2017; Smith, 2009; Hansen and Bartoszek, 2012]. Again, we centred and standardized the volumetric data for each brain subdivision prior to analysis. We then used the R package *phylolm* [Tung Ho and Ane, 2014] to generate linear models of each brain subdivision against SVL. As a post hoc analysis, we compared the residuals of each linear model using repeated-measures ANOVA. We also used phylogenetic linear models to determine whether any lateralization has evolved in brain subdivision volume. We generated models of left- versus right-hemisphere volumes for each brain subdivision, and compared the residuals of these linear regressions with repeated-measures ANOVA, as for our previous analysis.

We measured the phylogenetic signal with Blomberg's *K* statistic for each brain subdivision, in order to compare their relative lability with respect to each other. We also used the multivariate generalization of the K statistic (K_{mult} [Adams, 2014]), in order to test for the phylogenetic signal in all brain variables and in all body variables, as a comparison to the evolutionary lability of brain and

body morphology as whole structures. We used the R package *geomorph* [Adams and Otárola Castillo, 2013] to obtain measures of K_{mult} for the brain and body. We used the R package *picante* [Kembel et al., 2010] to calculate Blomberg's *K* for overall brain volume, each brain subdivision, our morphological measures of body shape, and ecomorph. We used a two-tailed Student *t* test to compare the Blomberg's *K* values for brain and body morphology, to determine whether there is a difference in evolutionary lability between brains and bodies. We conducted these analyses with both uncorrected morphological data and data that had been size-corrected according to Revell [2009]. Brain subdivisions were size-corrected to whole-brain volume while whole-brain volume and all body measurements were size-corrected to SVL. Furthermore, all further analyses were performed using size-corrected data unless otherwise specified.

To determine whether there are morphological traits, either in the body or brain, that are associated with ecomorph in *Ctenophorus*, we used phylogenetically corrected principal-components analysis (pPCA) and the R package *phytools* [Revell, 2011]. We assigned each species to an ecomorph, based on previous reports [Greer, 1989; Melville et al., 2001; Thompson and Withers, 2005b], and compared the clustering of species in the brain and body morphology pPCAs to determine whether ecomorphs have consistently different brain and body shapes. We then verified our findings using phylogenetically controlled ANOVAs of ecomorph against each brain subdivision using the R packages *geomorph* [Adams and Otárola Castillo, 2013] and *phytools* [Revell, 2011].

Finally, to estimate the ecomorph and associated brain structure of the ancestral *Ctenophorus*, we conducted an ancestral-state reconstruction of ecomorph in *Ctenophorus* using phytools [Revell, 2011]. In order to estimate the ancestral *Ctenophorus* ecomorph more accurately, we included in this analysis all species in the *C. nuchalis* group, not just those for which we have brain morphometry data. We pruned the original (Chen et al. [2012]) phylogeny to create a phylogeny of the central netted dragon (*C. nuchalis*) sp. group. Using McLean et al. [2013], we estimated the position of the Barrier Range dragon (*C. mirrityana*) on this phylogeny, resulting in a phylogeny of the entire central netted dragon species group. We repeated this analysis using the pruned Chen et al. [2012] phylogeny alone to confirm our results in the absence of the manually added tip. All new data used in this study is available in ESM 1.

Results

Models and Rates of Brain Evolution

We compared the AIC values for each brain subdivision under 5 models of brain evolution, and found that for most brain subdivisions, the Brownian motion evolutionary model fit our data best (Table 1). AIC values for the early-burst model were in some cases lower than the AIC values for Brownian motion. In these cases, the Brownian motion model had the second-lowest AIC values. Based on these results, we consider the Brownian motion model to be the best-fit model for explaining the patterns of brain evolution in *Ctenophorus*.

Table 1. AIC values for brain evolution under different evolutionary models

	BM	OU1	OU3	EB	Kappa	WN
Brain	**409**	412	44,374	**409**	412	411
Telencephalon	377	381	5,139	**373**	381	380
Diencephalon	**343**	346	715	**343**	346	345
Tectum	**356**	360	1,373	357	360	359
Tegmentum	**322**	326	392	324	326	324
Cerebellum	326	329	416	**325**	329	328
Rhombencephalon	**361**	364	1,731	**361**	364	363

The lowest AIC value, indicating the most likely model of brain evolution, is indicated in bold type. Brownian motion (BM) is most frequently the most likely model; however, early-burst (EB) is almost equally likely. OU, Ornstein-Uhlenbeck; WN, white noise.

The simulated rates of shape evolution for the brain and the body datasets showed no significant differences. The rates (R) and probabilities (*p*) of rates being significantly different between brains and bodies for the 3 analyses are as follows: all brain versus all body variables: $R_{brain} = 0.004$, $R_{body} = 0.005$, $p = 1.00$; whole-brain volume versus SVL: $R_{brain} = 0.004$, $R_{body} = 0.005$, $p = 0.30$; size-corrected brain versus size-corrected body variables: $R_{brain} = 0.004$, $R_{body} = 0.005$, $p = 1.00$. These results indicate that evolutionary rates are comparable between these 2 phenotypic datasets.

Evolution of Brain Subdivision Volume with Respect to Body Size

The volumes of all brain subdivisions were directly correlated with SVL. The slopes of all models approximated $b = 1$ and all confidence intervals included $b = 1$, indicating that all brain subdivisions evolved in almost perfect proportion to each other (Fig. 2). All models were significant to the $p < 0.0001$ level. Furthermore, a post hoc repeated-measures ANOVA of the residuals of each brain subdivision showed that there were no differences between subdivisions ($F_{5, 65} = 0.44$, $p = 0.82$), indicating that all brain subdivisions have the same amount of evolutionary lability with respect to body size.

Bilateral Asymmetry between Brain Subdivisions

The left and right hemispheres of each brain subdivision are evolving in concert, as the slopes of all models approximated $b = 1$ and the confidence intervals for all slopes included $b = 1$ (Fig. 3). All models were significant

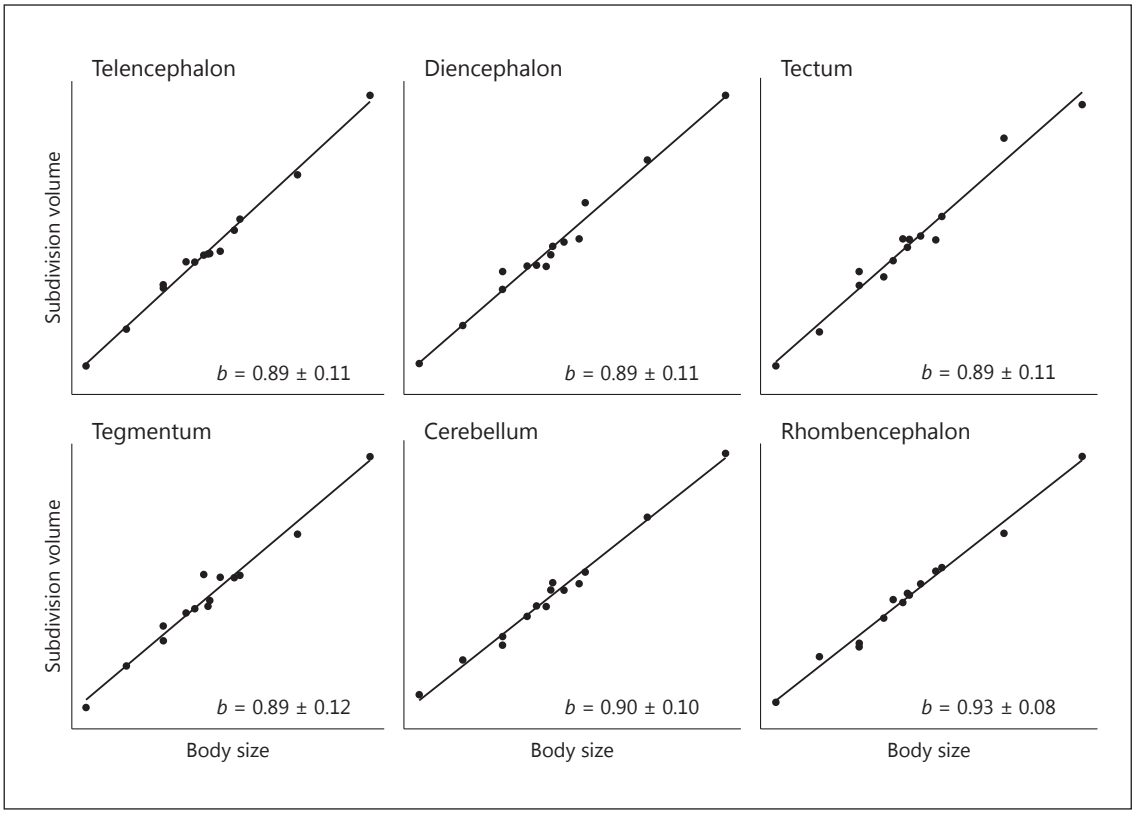

Fig. 2. The relationship between brain subdivision volume and body size. Using phylogenetically controlled linear models, we found that the volumes of all brain subdivisions strongly correlate with body size ($p < 0.0001$ for all subdivisions), and that the slopes (b) approximate 1 in all cases. Values of b for each brain subdivision ± 95% confidence intervals are supplied. Note that all values have been normalized and centred and therefore axis units are arbitrary.

to the $p < 0.0001$ level. Furthermore, a post hoc repeated-measures ANOVA comparing the linear model residuals revealed no differences between brain subdivisions in the level of symmetrical variation between species ($F_{5, 65} = 0.22$, $p = 0.95$). Therefore, we conclude that the left and right hemisphere subdivisions of the *Ctenophorus* brain evolve symmetrically.

Evolutionary Lability

Using the K_{mult} statistic, we found that overall brain morphology ($K = 1.23$, $p = 0.008$) is more evolutionarily stable than body morphology ($K = 0.98$, $p = 0.048$). This result was confirmed by calculating values of K individually for each brain subdivision and body region (t test, $t_{20} = 3.47$, $p = 0.002$; Table 2). However, ecomorph ($K = 1.58$, $p = 0.002$) was far more stable than either brain or body morphology.

The evolutionary signal in brain morphology is entirely due to the evolution of brain size. When K_{mult} was calculated for the size-controlled values of brain morphology, it was no longer significant ($K = 0.63$, $p = 0.705$) and when calculated for each subdivision individually, no brain subdivision had a significant value of K ($p > 0.05$ in all cases; Table 2). In contrast, K_{mult} for body morphology remained significant when size-controlled ($K = 1.06$, $p = 0.042$). When Blomberg's K was calculated for each body measure individually, most morphological measures were also no longer significant ($p > 0.05$; Table 2). However, head length, front- and hind-toe lengths, hind forearm length, and tail length showed a phylogenetic signal independent of body size. Only these measures also showed decreased phylogenetic lability in Blomberg's K values compared to the raw values. This suggests that the phylogenetic variation in these measures that is independent of body size is less evolutionarily labile than the phylogenetic variation that is associated with body size. Stated another way, it is easier for body regions to change size in concert with body size than it is to change size independent of body size.

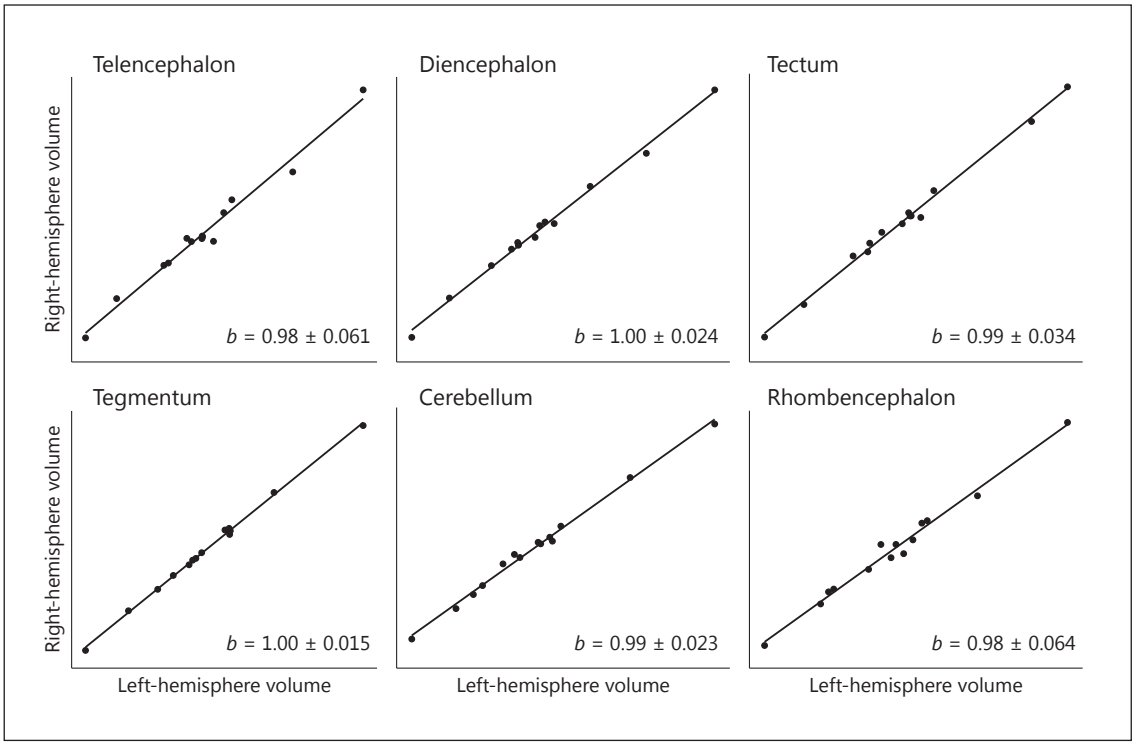

Fig. 3. Lateralization in the *Ctenophorus* brain. Phylogenetically controlled linear models comparing the left and right hemispheres of each brain subdivision demonstrate strong conservation of bilateral symmetry in the brains of *Ctenophorus* dragons. Slopes (*b*) are indicated for each model ± 95% confidence intervals. Note that all volumes have been normalized and centred and therefore axis units are arbitrary.

Relationship between Ecomorph, Morphology, and Brain Anatomy

Phylogenetically controlled pPCAs of size-independent body and brain morphology revealed that both segregate according to ecomorph (Fig. 4a, b). Plotting PC1 versus PC2 of brain morphology shows that burrowers have distinct brain morphology compared to sprinters and rock dwellers (Fig. 4a). Sprinter and rock dweller brains, however, are not distinct from each other. With respect to body morphology (Fig. 4b), burrowers, sprinters, and rock dwellers are all distinct, but burrowers are more morphologically distant from sprinters and rock dwellers than the latter 2 are from each other. Eigenvalues, variances, and loadings for the first 5 principal components are available in ESM 2.

To further examine the relationship between brain morphology and ecomorph, we performed phylogenetically corrected ANOVAs comparing brain and body morphology between ecomorphs. We used size-corrected values for all measures, to eliminate the effects of body size on both brain and body morphology. We found that there was a significant effect of ecomorph on brain morphology ($F_{1, 12} = 1.94$, $p = 0.018$) but not on body morphology ($F_{2, 11} = 1.11$, $p = 0.122$). Therefore, although body shape appears to segregate according to ecomorph in pPCA analysis, as previous studies have found [Thompson and Withers, 2005a, b], formal statistical analysis did not detect significant differences between ecomorphs in this case.

We next examined which brain subdivisions differ in volume between the different ecomorphs. Since our results indicate that burrowers have brain morphology distinct from that of sprinters and rock dwellers, but that the latter 2 do not differ from each other, we collapsed our ecomorph categories into "burrower" and "sprinter/rock dweller." Using phylogenetically corrected ANOVAs, we found that the volume of the optic tectum is larger ($T_{2, 12} = -3.62$, $p = 0.0035$) and the rhombencephalon smaller ($T_{2, 12} = 3.23$, $p = 0.0072$), in burrowers compared to sprinters and rock dwellers (Fig. 5). We replicated these analyses without collapsing the ecomorph categories, and the results are qualitatively identical (ESM 3).

Table 2. Blomberg's *K* values for brain and body morphology

Class	Measure	Raw		Size-independent	
		K	*p*	*K*	*p*
Brain morphology	Whole brain	**1.12**	**0.010**	0.63	0.718
	Telencephalon	**1.13**	**0.018**	0.50	0.941
	Diencephalon	**1.11**	**0.017**	0.84	0.248
	Tectum	**1.15**	**0.013**	1.00	0.081
	Tegmentum	**1.09**	**0.017**	0.82	0.362
	Cerebellum	**1.13**	**0.011**	0.73	0.468
	Rhombencephalon	**1.09**	**0.012**	0.94	0.150
Body morphology	Weight	**1.10**	**0.029**	–	–
	Snout-to-vent length	**1.07**	**0.032**	–	–
	Head length	**1.08**	**0.019**	**1.41**	**0.003**
	Head width	**1.11**	**0.014**	0.98	0.090
	Front toe	**1.17**	**0.009**	**1.17**	**0.046**
	Front palm	**1.06**	**0.027**	1.06	0.126
	Front forearm	**1.07**	**0.037**	0.81	0.290
	Front upper arm	**1.12**	**0.020**	0.90	0245
	Interlimb length	**1.08**	**0.034**	0.77	0.362
	Hind toe	**0.99**	**0.046**	**1.15**	**0.048**
	Hind palm	0.96	0.067	0.96	0.274
	Hind forearm	**1.04**	**0.019**	**1.20**	**0.044**
	Hind upper arm	**1.02**	**0.025**	1.07	0.096
	Hip height	1.06	0.062	0.73	0.524
	Tail length	0.98	0.055	**1.19**	**0.028**

Size-independent measures are residuals from regressions of the raw measures for each subdivision against body size, as estimated by snout-to-vent length. Removing variation due to size eliminates phylogenetic signal for most measures. Values in bold are significant at the $p < 0.05$ level.

Estimating the Ancestral Ctenophorus

Finally, we estimated the ancestral ecomorph of the *Ctenophorus* genus in order to predict the ancestral brain morphology of the genus. The ancestral-state reconstruction predicted that *Ctenophorus* was a burrower with a 65% probability, suggesting a relatively large tectum and small rhombencephalon is the ancestral *Ctenophorus* brain shape. According to this analysis, there was a 27% probability that the ancestral *Ctenophorus* was a rock dweller and an 8% chance it was a sprinter. An ancestral-state reconstruction without the Barrier Ranges dragon (*C. mirrityana*) confirms these results ($p_{\text{burrower}} = 64\%$, $p_{\text{rock dweller}} = 27\%$, $p_{\text{sprinter}} = 9\%$). Therefore, we conclude that the mostly likely scenario is that the ancestral *Ctenophorus* was a burrower, and that the sprinter and rock dweller ecomorphs each emerged twice within this radiation (Fig. 6).

Discussion

We found support for both concerted and mosaic brain evolution among dragon lizards. As expected, the most important factor predicting brain volume and the volumes of all the major neural subdivisions was body size. We found that all brain subdivisions are evolving in near-perfect concert with respect to body size. We also found evidence for mosaic brain evolution with respect to ecomorph. In this case, the tectum was larger in species of the "burrower" ecomorph, which dig and shelter in burrows, than in the "sprinter" and "rock dweller" ecomorphs, which shelter in grass hummocks and rock crevices respectively. The rhombencephalon (excluding the cerebellum) was smaller in burrowers than in sprinters and rock dwellers. Overall, we found evidence for both concerted and mosaic brain evolution occurring simultaneously in the same structures, but in response to different selection pressures. We discuss each of these findings in turn.

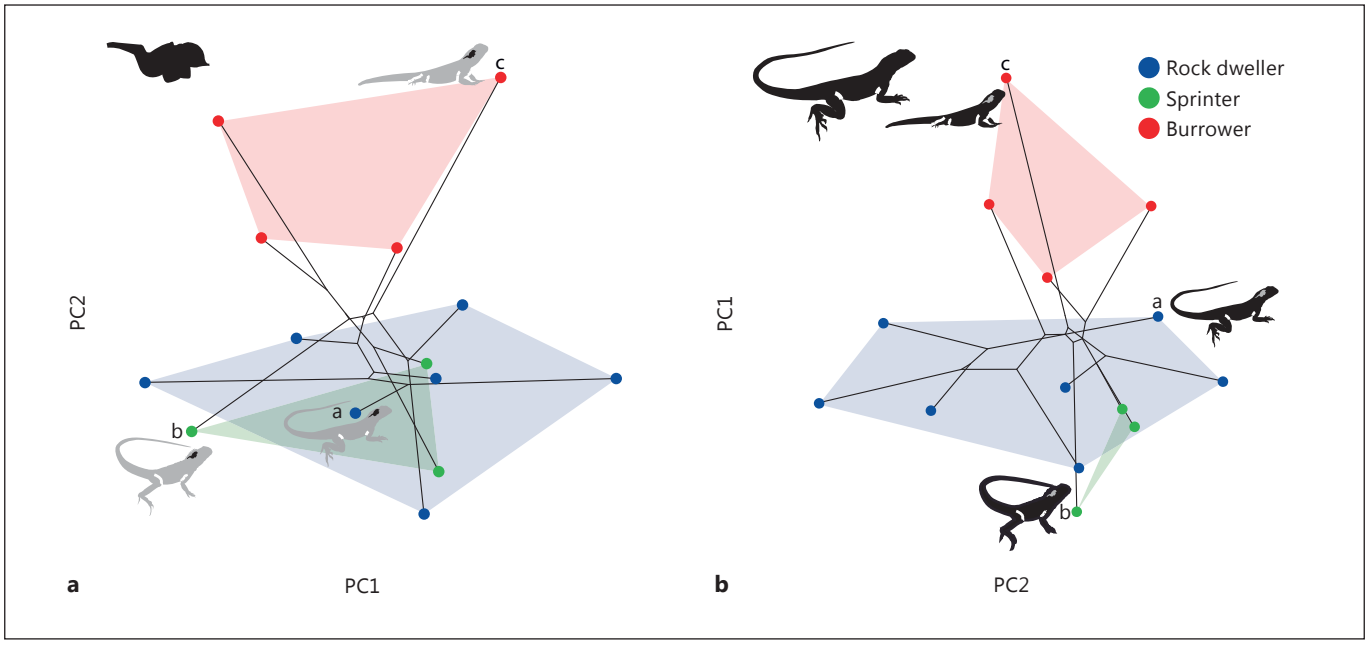

Fig. 4. Phylogenetically corrected principal-components analysis (pPCA) of body and brain morphology. Both the brain (**a**) and body (**b**) morphology pPCAs segregate species into ecomorph. Body morphology is distinct between all 3 ecomorphs, while brain morphology is distinct only in burrowers. Lines indicate phylogenetic relatedness.

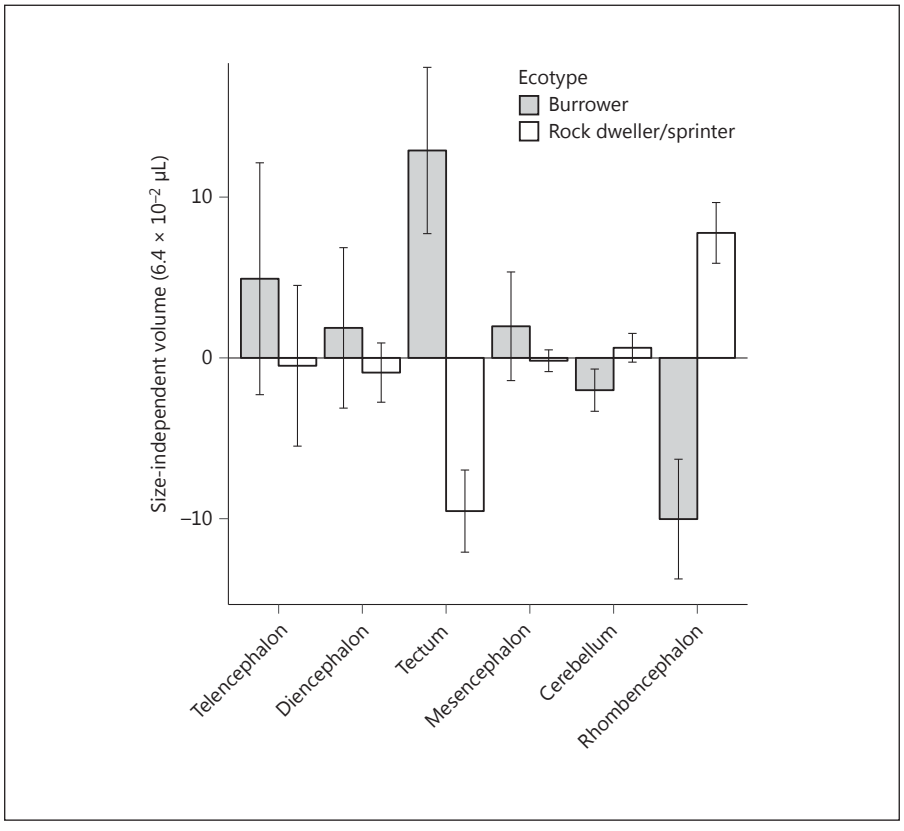

Fig. 5. The optic tectum is larger and the rhombencephalon smaller in burrowers when compared to sprinters and rock dwellers. The remaining 4 brain subdivisions do not differ in volume between ecomorphs. This exemplifies a mosaic pattern of brain evolution. Bars are size-independent means ± standard error.

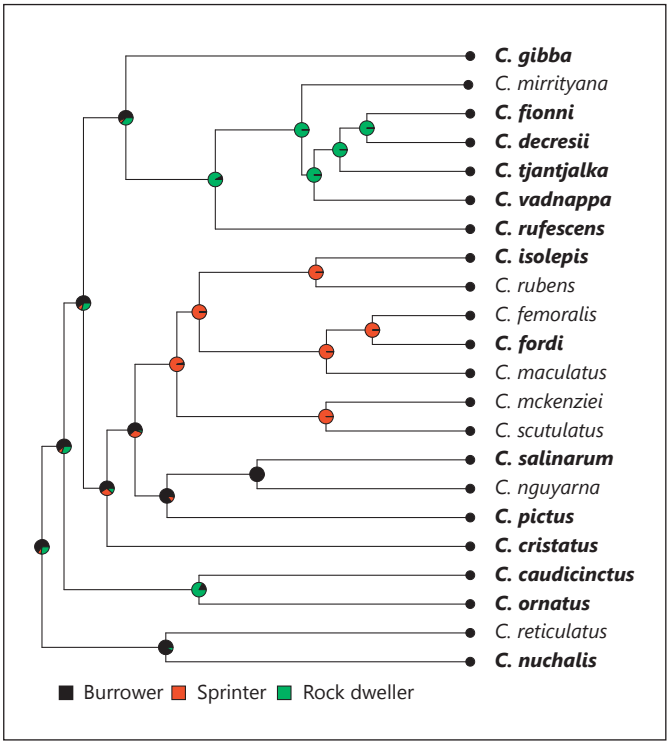

Fig. 6. Ancestral ecomorph reconstruction for the central netted dragon (*C. nuchalis*) sp. group of the genus *Ctenophorus*. Ancestral-state reconstruction of ecomorph shows that the "burrower" ecomorph is the most likely ancestor of the clade. "Sprinter" and "rock dweller" ecomorphs each emerged twice, resulting in 2 extant clades of sprinters and rock dwellers and 3 extant clades of burrowers. All ecomorph clades are represented by at least 1 species (denoted in bold type) in this study.

We found a concerted pattern of brain evolution in dragons with respect to body size. We studied a group of closely related lizards because it has previously been reported that the relationship between brain and body size is weaker amongst closely related species [van Dongen, 1998]. We hypothesized that investigating close relatives would most easily reveal other selective pressures that act on brain volume. However, almost all the variation in the volumes of the 6 brain subdivisions correlated with body size in *Ctenophorus*. In fact, the relationships between the volumes of all brain subdivisions and brain volume is 1:1, showing that the subdivisions of the *Ctenophorus* brain are evolving in perfect concert with each other, relative to body size. We hypothesized that the smaller regions, such as the cerebellum and tectum, may be less constrained by changes in body size, and would therefore show either a linear relationship with brain size <1:1, or increased lability with respect to brain size, but we did not find any support for this hypothesis.

Despite the strong relationship between brain structure and body size, we did find variation in brain morphology that correlated with another trait: ecomorph. The classical adaptive radiation studies on ecomorph divergence in *Anolis* lizards reveal strong, repeated, convergent evolution across island systems [Losos et al., 1998; Langerhans et al., 2006]. Interestingly, while *Anolis* ecomorphs have evolved many times independently, there is no parallel evolution between ecomorph and brain structure [Powell and Leal, 2012]. In other words, ecomorph does not predict brain structure in *Anolis*.

In contrast to *Anolis*, we found that ecomorph does impact brain evolution in *Ctenophorus*. Specifically, we found that ecomorph is associated with variation in tectum and rhombencephalon volume. We found that the tectum was larger in burrowers than in sprinters and rock dwellers. The tectum is the primary neural processing centre for visual information but also receives input from several other sensory modalities (note, however, that the torus semicircularis, the primarily auditory processing region, is not part of the tectum). Therefore, it is difficult to draw functional conclusions. Previous works have also noted interspecific variation in the optic tectum in reptiles, and have similarly struggled to explain why such a variation exists [Carl Huber and Crosby, 1933; Senn, 1966; Platel, 1976]. Therefore, selective, specialized evolutionary changes in tectum volume appear to be relatively common in squamates, and yet are very poorly understood. This may represent a novel opportunity to investigate how selection on different sensory modalities results in changes to the way the brain processes and integrates information from these different modalities.

We also found that the volume of the rhombencephalon, excluding the cerebellum, was smaller in burrowers than in sprinters and rock dwellers. The rhombencephalon is the most conserved neural subdivision across vertebrates [Gonzalez-Voyer et al., 2009], and has been used as a "baseline" brain structure with which to measure mosaic brain evolution in other subdivisions [Striedter, 2005]. Therefore, we expected it to be the least evolutionarily labile structure in the dragon brain. Instead, we found that it is the most labile brain subdivision, with the lowest Blomberg's *K* value and volumetric changes correlated with ecomorph. The rhombencephalon contains many nuclei involved in sensory processing across modalities, and we hypothesize that ecomorph-dependent variation in the rhombencephalon may be due to selection on sensory modalities. As the rhombencephalon

contains nuclei important for processing sensory modalities other than vision, change in rhombencephalic and tectal volumes could represent evolutionary trade-offs between sensory modalities [Wylie et al., 2015]. Alternatively, visual nuclei can evolve as a mosaic [Gutiérrez-Ibáñez et al., 2014], and therefore the contrasting variations that we found in the rhombencephalon and tectum may represent various changes within the visual processing system. As sensory processing nuclei are generally small compared to the volumes of the subdivisions in which they are located, variations in the volume of individual nuclei are unlikely to result in detectable volumetric changes in the entire subdivision unless several nuclei change volume in concert. This may be the case when sensory modalities are under directional selection. We hypothesize that, in *Ctenophorus*, there is differential selection in sensory modalities between burrowers and sprinters/rock dwellers.

The telencephalon, diencephalon, tegmentum, and cerebellum did not vary with ecomorph. The telencephalon, diencephalon, and tegmentum all contain a wide array of nuclei that perform many varied functions, and it is not surprising that there is not a consistent difference between ecomorphs in the volumes of these subdivisions. However, the cerebellum was described by Platel [1976] as one of the two most evolutionarily labile brain subdivisions in squamates (the other being the tectum). We only detected variations in cerebellum volume with body size, again supporting a more concerted model of brain evolution. This difference in conclusions may be due to Platel's broader scope across the squamates; although he did not perform a formal analysis, he associated the variations in cerebellum volume with locomotion. Species capable of bipedal locomotion or that are arboreal have the largest cerebella, while species without legs have the smallest cerebella. All *Ctenophorus* dragons are capable of bipedal locomotion [Clemente et al., 2008; Clemente, 2014] and therefore, according to Platel's hypothesis, we expect them to all have well developed cerebella.

We did not find differences between the 2 hemispheres in any brain subdivision. The lizard brain is well known for being heavily lateralized [Deckel, 1995, 1997, 1998; Deckel and Jevitts, 1997; Smith et al., 1997; Deckel et al., 1998; Deckel and Fuqua, 1998; Dávila et al., 2000; Bonati et al., 2008; Csermely et al., 2010; Bonati and Csermely, 2012]. However, we predicted that these lateralizations are at the levels of individual nuclei, and were unable to detect them at the gross anatomical level we examined.

We have shown that the same brain structures can evolve simultaneously independently and in concert. Furthermore, we have shown that whether concerted or mosaic brain evolution is detected in a particular system may depend more on the specific hypothesis and evolutionary pressures selected for study than the species or brain structures studied. Further research is needed to confirm whether the patterns of concerted and mosaic brain evolution that we found are consistent across a wider range of squamate species and with respect to a wider variety of relevant characteristics. We also need to understand the underlying structural changes within each of the subdivisions to start to unravel both the causes (specifically, what selection pressures are inducing these changes) and consequences (on brain function, cognition, and behaviour) of evolutionary changes in the brain. Nonetheless, this study is an important step forward in our understanding of brain evolution.

Acknowledgments

We thank the facilities and the scientific and technical assistance of the National Imaging Facility, Western Sydney University and University of Queensland Nodes. B. Moroney (Nanoscale Group, Western Sydney University) designed the lizard brain holder that made the MRI scanning possible. This work was supported by grants to D.H. from the National Science and Engineering Council of Canada, The Australian National University, and The National Imaging Facility of Australia; and by grants to M.J.W. and J.S.K. from the Australian Research Council.

Disclosure Statement

The authors declare no conflicts of interest.

References

Adams DC (2014): A generalized K statistic for estimating phylogenetic signal from shape and other high-dimensional multivariate data. Syst Biol 63:685–697.

Adams DC, Otárola Castillo E (2013): geomorph: an R package for the collection and analysis of geometric morphometric shape data. Methods Ecol Evol 4:393–399.

Barton RA, Harvey PH (2000): Mosaic evolution of brain structure in mammals. Nature 405: 1055–1058.

Boire D, Baron G (1994): Allometric comparison of brain and main brain subdivisions in birds. J Hirnforsch 35:49–66.

Bonati B, Csermely D (2012): Lateralization in lizards: evidence of presence in several contexts; in Csermely D, Regolin L (eds): Behavioral Lateralization in Vertebrates. Berlin, Heidelberg, Springer, pp 25–38.

Bonati B, Csermely D, Romani R (2008): Lateralization in the predatory behaviour of the common wall lizard (*Podarcis muralis*). Behav Process 79:171–174.
Brown WM (2001): Natural selection of mammalian brain components. TREE 16:471–473.
Butler AB, Hodos W (2005): Comparative Vertebrate Neuroanatomy: Evolution and Adaptation, ed 2. Hoboken, NJ, Wiley.
Butler MA, King AA, Crespi BJ (2004): Phylogenetic comparative analysis: a modeling approach for adaptive evolution. Am Nat 164: 683–695.
Butler AB, Northcutt RG (1973): Architectonic studies of the diencephalon of *Iguana iguana* (Linnaeus). J Comp Neurol 149:439–462.
Carl Huber G, Crosby EC (1933): The reptilian optic tectum. J Comp Neurol 57:57–163.
Charvet CJ, Striedter GF, Finlay BL (2011): Evo-devo and brain scaling: candidate developmental mechanisms for variation and constancy in vertebrate brain evolution. Brain Behav Evol 78:248–257.
Chen I-P, Stuart-Fox DM, Hugall AF, Symonds MRE (2012): Sexual selection and the evolution of complex color patterns in dragon lizards. Evolution 66:3605–3614.
Clemente CJ (2014): The evolution of bipedal running in lizards suggests a consequential origin may be exploited in later lineages. Evolution 68:2171–2183.
Clemente CJ, Withers PC, Thompson GG, Lloyd D (2008): Why go bipedal? Locomotion and morphology in Australian agamid lizards. J Exp Biol 211:2058–2065.
Collins DL, Neelin P, Peters TM, Evans AC (1994): Automatic 3D intersubject registration of MR volumetric data in standardized Talairach space. J Comp Assist Tomog 18: 192.
Cruce JAF (1974): A cytoarchitectonic study of the diencephalon of the tegu lizard, *Tupinambis nigropunctatus*. J Comp Neurol 153:215–238.
Cruce WLR, Newman DB (1981): Brain stem origins of spinal projections in the lizard *Tupinambis nigropunctatus*. J Comp Neurol 198:185–207.
Csermely D, Bonati B, Romani R (2010): Lateralisation in a detour test in the common wall lizard (*Podarcis muralis*). Laterality 15:535–547.
Dávila JC, Guirado S, Puelles L (2000): Expression of calcium-binding proteins in the diencephalon of the lizard *Psammodromus algirus*. J Comp Neurol 427:67–92.
Deckel AW (1995): Laterality of aggressive responses in *Anolis*. J Exp Zool 272:194–200.
Deckel AW (1997): Effects of alcohol consumption on lateralized aggression in *Anolis carolinensis*. Brain Res 756:96–105.
Deckel AW (1998): Hemispheric control of territorial aggression in *Anolis carolinensis*: effects of mild stress. Brain Behav Evol 51:33–39.
Deckel AW, Fuqua L (1998): Effects of serotonergic drugs on lateralized aggression and aggressive displays in *Anolis carolinensis*. Behav Brain Res 95:227–232.
Deckel AW, Jevitts E (1997): Left vs. right-hemisphere regulation of aggressive behaviors in *Anolis carolinensis*: effects of eye-patching and fluoxetine administration. J Exp Zool 278:9–21.
Deckel AW, Lillaney R, Ronan PJ, Summers CH (1998): Lateralized effects of ethanol on aggression and serotonergic systems in *Anolis carolinensis*. Brain Res 807:38–46.
Del Corral JM, Miralles A, Nicolau MC, Planas B, Rial RV (1990): Stereotaxic atlas for the lizard *Gallotia galloti*. Prog Neurobiol 34:185–196.
Denton JSS, Adams DC (2015): A new phylogenetic test for comparing multiple high-dimensional evolutionary rates suggests interplay of evolutionary rates and modularity in lantern fishes (Myctophiformes; Myctophidae). Evolution 69:2425–2440.
Dobson SD, Sherwood CC (2011): Mosaic evolution of brainstem motor nuclei in Catarrhine primates. Anat Res Internat 2011:1–5.
Finlay BL, Darlington RB (1995): Linked regularities in the development and evolution of mammalian brains. Science 268:1578–1584.
Finlay BL, Hinz F, Darlington RB (2011): Mapping behavioural evolution onto brain evolution: the strategic roles of conserved organization in individuals and species. Phil Trans R Soc B 366:2111–2123.
Greenberg N (1982): A forebrain atlas and stereotaxic technique for the lizard, *Anolis carolinensis*. J Morphol 174:217–236.
Gonzalez-Voyer A, Winberg S, Kolm N (2009): Brain structure evolution in a basal vertebrate clade: evidence from phylogenetic comparative analysis of cichlid fishes. BMC Evol Biol 9:238.
Greer AE (1989): Agamidae – dragon lizards; in: The Biology and Evolution of Australian Lizards. Surrey, Beatty.
Gutiérrez-Ibáñez C, Iwaniuk AN, Moore BA, Fernández-Juricic E, Corfield JR, Krilow JM, et al (2014): Mosaic and concerted evolution in the visual system of birds. PLoS One 9:e90102.
Hager R, Lu L, Rosen GD, Williams RW (2012): Genetic architecture supports mosaic brain evolution and independent brain and body size regulation. Nat Comms 3:1079.
Hamilton AJ, May RM, Waters EK (2015): Zoology: here be dragons. Nature 520:42–43.
Hansen TF, Bartoszek K (2012): Interpreting the evolutionary regression: the interplay between observational and biological errors in phylogenetic comparative studies. Syst Biol 61:413–425.
Harmon LJ, Weir JT, Brock CD, Glor RE, Challenger W (2008): GEIGER: investigating evolutionary radiations. Bioinformatics 24:129–131.
Hoops D (2015): A perfusion protocol for lizards, including a method for brain removal. MethodsX 2:165–173.
Hoops D, Ullmann JFP, Janke AL, Vidal-García M, Stait Gardner T, Dwihapsari Y, et al (2016): Sexual selection predicts brain structure in dragon lizards. J Evol Biol 30:244–256.
Iwaniuk AN, Dean KM, Nelson JE (2004): A mosaic pattern characterizes the evolution of the avian brain. Proc R Soc B 271:S148–S151.
Janke AL, Ullmann JFP (2015): Robust methods to create ex vivo minimum deformation atlases for brain mapping. Methods 73:18–26.
Kandel E (2013): Principles of Neural Science, ed 5. New York, NY, McGraw-Hill Education.
Kembel SW, Cowan PD, Helmus MR, Cornwell WK, Morlon H, Ackerly DD, et al (2010): Picante: R tools for integrating phylogenies and ecology. Bioinformatics 26:1463–1464.
Kilmer JT, Rodríguez RL (2017): Ordinary least squares regression is indicated for studies of allometry. J Evol Biol 30:4–12.
Kotrschal K, van Staaden MJ, Huber R (1998): Fish brains: evolution and environmental relationships. Rev Fish Biol Fish 8:373–408.
Langerhans RB, Knouft JH, Losos J (2006): Shared and unique features of diversification in Greater Antillean *Anolis* ecomorphs. Evolution 60:362–369.
Lanuza E, Halpern M (1997): Afferent and efferent connections of the nucleus sphericus in the snake *Thamnophis sirtalis*: convergence of olfactory and vomeronasal information in the lateral cortex and the amygdala. J Comp Neurol 385:627–640.
Losos J, Jackman TR, Larson A, de Queiroz K, Rodríguez-Schettino L (1998): Contingency and determinism in replicated adaptive radiations of island lizards. Science 279:2115–2118.
McLean CA, Moussalli A, Sass S, Stuart-Fox DM (2013): Taxonomic assessment of the *Ctenophorus decresii* complex (Reptilia: Agamidae) reveals a new species of dragon lizard from western New South Wales. Rec Aust Mus 65:51–63.
Medina LM, Martí E, Artero C, Fasolo A, Puelles L (1992): Distribution of neuropeptide Y-like immunoreactivity in the brain of the lizard *Gallotia galloti*. J Comp Neurol 319:387–405.
Melville J, Schulte JA, Larson A (2001): A molecular phylogenetic study of ecological diversification in the Australian lizard genus *Ctenophorus*. J Exp Zool 291:339–353.
Northcutt RG (1967): Architectonic studies of the telencephalon of *Iguana iguana*. J Comp Neurol 130:109–147.
Northcutt RG (2013): Variation in reptilian brains and cognition. Brain Behav Evol 82: 45–54.
Paradis E, Claude J, Strimmer K (2004): APE: Analyses of phylogenetics and evolution in R language. Bioinformatics 20:289–290.
Platel MR (1976): Analyse volumétrique comparée des principales subdivisions encéphaliques chez les reptiles sauriens. J Hirnforsch 17:513–537.

Powell BJ, Leal M (2012): Brain evolution across the Puerto Rican anole radiation. Brain Behav Evol 80:170–180.
Powell BJ, Leal M (2014): Brain organization and habitat complexity in *Anolis* lizards. Brain Behav Evol 84:8–18.
R Core Team (2014): R: a language and environment for statistical computing. Vienna, R Foundation for Statistical Computing.
Revell LJ (2009): Size-correction and principal components for interspecific comparative studies. Evolution 63:3258–3268.
Revell LJ (2011): phytools: an R package for phylogenetic comparative biology (and other things). Methods Ecol Evol 3:217–223.
Schwab ME (1979): Variation in the Rhombencephalon; in: Biology of the Reptilia: Neurology B. Academic Press, 1979, pp 201–242.
Senn DG (1966): Über das optische System im Gehirn squamater Reptilien. Acta Anat 65: 1–87.
Sled JG, Zijdenbos AP, Evans AC (1998): A nonparametric method for automatic correction of intensity nonuniformity in MRI data. IEEE Trans Med Imaging 17:87–97.
Smeets WJAJ, Hoogland PV, Lohman AHM (1986): A forebrain atlas of the lizard *Gekko gecko*. J Comp Neurol 254:1–19.
Smith MT, Moore FL, Mason RT (1997): Neuroanatomical distribution of chicken-I gonadotropin-releasing hormone (cGnRH-I) in the brain of the male red-sided garter snake. Brain Behav Evol 49:137–148.
Smith RJ (2009): Use and misuse of the reduced major axis for line-fitting. Am J Phys Anthropol 140:476–486.
Striedter GF (2005): Principles of Brain Evolution. Sunderland, MA, Sinauer Associates.
ten Donkelaar HJ (1988): Evolution of the red nucleus and rubrospinal tract. Behav Brain Res 28:9–20.
ten Donkelaar HJ, Bangma GC, Barbas-Henry HA, Huizen R de BV, Wolters JG: The Brain Stem in a Lizard, *Varanus exanthematicus*. Springer, 2012.
Thompson GG, Withers PC (2005a): Shape of Western Australian dragon lizards (Agamidae). Amphib-Reptil 26:73–85.
Thompson GG, Withers PC (2005b): The relationship between size-free body shape and choice of retreat for Western Australian *Ctenophorus* (Agamidae) dragon lizards. Amphib-Reptil 26:65–72.
Thompson GG, Withers PC (2005d): Size-free shape differences between male and female Western Australian dragon lizards (Agamidae). Amphib-Reptil 26:55–63.
Tung Ho LS, Ane C (2014): A linear-time algorithm for Gaussian and non-Gaussian trait evolution models. Syst Biol 63:397–408.
Ulinski PS, Peterson EH (1981): Patterns of olfactory projections in the desert iguana, *Dipsosaurus dorsalis*. J Morphol 168:189–227.
Ullmann JFP, Cowin G, Collin SP (2010): Magnetic resonance microscopy of the barramundi (*Lates calcarifer*) brain. J Morphol 271: 1446–1456.
Ullmann JFP, Janke AL, Reutens D, Watson C (2015): Development of MRI-based atlases of non-human brains. J Comp Neurol 523:391–405.
van Dongen PAM (1998): Brain size in vertebrates; in Nicholson C (ed): The Central Nervous System of Vertebrates. Berlin, Springer, pp 2100–2134.
Whiting BA, Barton RA (2003): The evolution of the cortico-cerebellar complex in primates: anatomical connections predict patterns of correlated evolution. J Hum Evol 44:3–10.
Wolters JG, Donkelaar ten HJ, Steinbusch H, Verhofstad A (1985): Distribution of serotonin in the brain-stem and spinal cord of the lizard Varanus exanthematicus: an immunohistochemical study. Neurosci 14:169–193.
Wolters JG, Donkelaar ten HJ, Verhofstad AA (1984): Distribution of catecholamines in the brain stem and spinal cord of the lizard *Varanus exanthematicus*: an immunohistochemical study based on the use of antibodies to tyrosine hydroxylase. Neurosci 13:469–493.
Wylie DR, Gutiérrez-Ibáñez C, Iwaniuk AN (2015): Integrating brain, behavior, and phylogeny to understand the evolution of sensory systems in birds. Front Neurosci 9:281.
Yopak KE, Lisney TJ, Darlington RB, Collin SP, Montgomery JC, Finlay BL (2010): A conserved pattern of brain scaling from sharks to primates. PNASI 107:12946–12951.